JOURNAL OF Materials CHEMISTRY

Porous properties of coprecipitated Al_2O_3–SiO_2 xerogels prepared from aluminium nitrate nonahydrate and tetraethylorthosilicate

Kiyoshi Okada,[a] Takahiro Tomita,[a] Yoshikazu Kameshima,[a] Atsuo Yasumori[a] and Kenneth J. D. MacKenzie†[b]

[a]*Department of Metallurgy and Ceramics Science, Tokyo Institute of Technology, O-okayama, Meguro, Tokyo 152–8552, Japan. E-mail: kokada@o.cc.titech.ac.jp*
[b]*The New Zealand Institute for Industrial Research and Development, Lower Hutt, New Zealand*

Received 22nd January 1999, Accepted 12th April 1999

Al_2O_3–SiO_2 xerogels with various chemical compositions have been prepared by coprecipitation and their porous properties investigated by nitrogen gas adsorption, transmission electron microscopy (TEM), small angle X-ray scattering (SAXS), and ^{29}Si and ^{27}Al magic angle spinning nuclear magnetic resonance (MAS NMR). The precipitates were formed by adding conc. aqueous ammonia to an ethanol solution of $Al(NO_3)_3 \cdot 9H_2O$ and $Si(OC_2H_5)_4$ (TEOS). The syntheses were performed both with and without added H_2O (H_2O/TEOS $\geqslant$ 18/1). The xerogels were dried and calcined at 300 °C for 4 h. The porous properties [specific surface area (S_A), pore volume (V_P) and pore size (r_P)] varied with their chemical composition, especially the SiO_2 rich xerogels. The experimental S_A values ranged from *ca.* 10 to 560 m^2g^{-1}, the V_P values from 0.02 to 1.55 ml g^{-1} and the r_P values from 2 to 34 nm. The addition of H_2O during the preparation markedly influenced the porous properties of the xerogels with SiO_2 rich composition. The structure and microtexture of the xerogels are discussed on the basis of the NMR, SAXS and TEM data.

Introduction

Amorphous aluminosilicates were used in large amounts as acid catalysts up to a few decades ago but they have now been largely replaced by zeolites,[1] which are microporous crystalline aluminosilicates. They are however increasingly finding new applications as membranes for separation of gas phases,[2] purification of water[3] and reactors,[4] adsorbents, humidity control materials,[5] and so on. For these applications, it is very important to control both the porous properties and the surface properties of the amorphous aluminosilicates. Amorphous aluminosilicates are also important as starting materials for synthesis of mullite ($Al_{4+2x}Si_{2-2x}O_{10-x}$) ceramics.[6] For this purpose, the homogeneity of the Al and Si components is a more important factor than the porous properties.

Of the various preparation methods for porous ceramics, sol–gel synthesis is one of the most practical, and is the subject of many papers on the preparation and properties of porous amorphous aluminosilicates. For the preparation of materials with good porous properties, the effect of the synthesis conditions [starting materials,[7] pH of solution,[8] solvents,[9] templates,[10] drying control chemical additives (DCCA),[11] *etc.*] have been examined mainly with respect to the chemical composition of the aluminosilicates. May *et al.*[7] examined the effect of starting with different aluminium alkoxides and found that the specific surface area of aluminosilicates increased with decreasing number of carbon atoms in the alkoxyl groups. De Witte and Uytterhoeven[8] used a preparation method involving precipitation from solutions of Na_4SiO_4 and $NaAlO_2$ at alkaline pH and also from $Si(OC_2H_5)_4$ (TEOS) and $Al(NO_3)_3 \cdot 9H_2O$ (ANN) solutions at acidic pH. They examined the effect of the final pH and Al content on the porous properties, which they found to vary with Al content, which they considered to determine the degree of incorporation of Al in the tetrahedral network and the subsequent changes in the condensation reactivity. Inagaki *et al.*[10] reported the effectiveness of organic templates in the formation and control of the size of mesopores in amorphous aluminosilicates. DCCA[11] was also reported to be effective in controlling the size of the mesopores which were formed in the spaces of the agglomerated fine particles during hydrolysis and drying.

In addition to controlling the porous properties, it is also important to design the appropriate surface chemical properties of aluminosilicates for use as catalysts, catalyst supports and adsorbents. The surface acidity of aluminosilicates is known to be related to the coordination of the Al atoms, which is also reported to vary with the preparation conditions. For example, De Witte *et al.*[11] reported that a DCCA such as formamide and/or dimethylformamide increased the tetrahedral Al coordination and gave rise to higher surface charge and acidity. For adsorbent materials, the interaction between adsorbate gas and adsorbent is very important and is related to the surface properties of the adsorbents. In aluminosilicates, the interaction with water vapor is expected to depend mainly on their surface chemical composition, because silica is well known to show typical hydrophobic character while alumina is typically hydrophilic. Okada *et al.*[5] reported that the average thickness of the adsorbed water vapor layer on the surface of aluminosilicates is a function of the surface chemistry as expected from the above consideration.

Despite the numerous reported studies of the porous properties and chemical properties of amorphous aluminosilicates, they are not well understood, especially the effect of changes in their chemical composition. We therefore prepared aluminosilicates of various chemical compositions by coprecipitation from an ethanol solution of TEOS and ANN using aqueous ammonia as the precipitant, and examined the porous properties of the products as a function of their chemical composition.

Experimental

Sample preparation

Al_2O_3–SiO_2 xerogels of various compositions were prepared by coprecipitation. The starting materials were reagent grade

---

†Present address: Department of Materials, Oxford University, Oxford, UK OX1 3PH.

aluminium nitrate nonahydrate [ANN; $Al(NO_3)_3{\cdot}9H_2O$] and tetraethylorthosilicate [TEOS; $Si(OC_2H_5)_4$]. The xerogels were prepared according to the experimental flow chart shown in Fig. 1. The concentration of total ANN and TEOS was adjusted to 1.2 mol l^{-1} in all the preparations. For the preparations without added water [Fig. 1(a)], measured amounts of ANN and TEOS were dissolved in absolute ethanol and stirred vigorously. In this preparation, the only H_2O in the solution arises from the hydration water of the ANN and therefore, the amount of H_2O is strongly dependent on the amount of ANN added. The amount of water in the composition not containing Al_2O_3 was very low, arising only from impurity H_2O in the ethanol and atmospheric moisture. The water in this sample is apparently insufficient for complete hydrolysis of TEOS. In the other SiO_2-rich compositions, the amount of H_2O is also considered to be insufficient for complete hydrolysis of TEOS because of the low H_2O/TEOS ratio; after stirring the solution for 3 h, 25 mass% aqueous ammonia solution (100 ml) was added rapidly to the solution with vigorous stirring. The precipitates were immediately dried using an evaporator at 60 °C for 2 h and subsequently dried at 110 °C for 15 h in an oven. After drying, they were calcined at 300 °C for 4 h to obtain the xerogels.

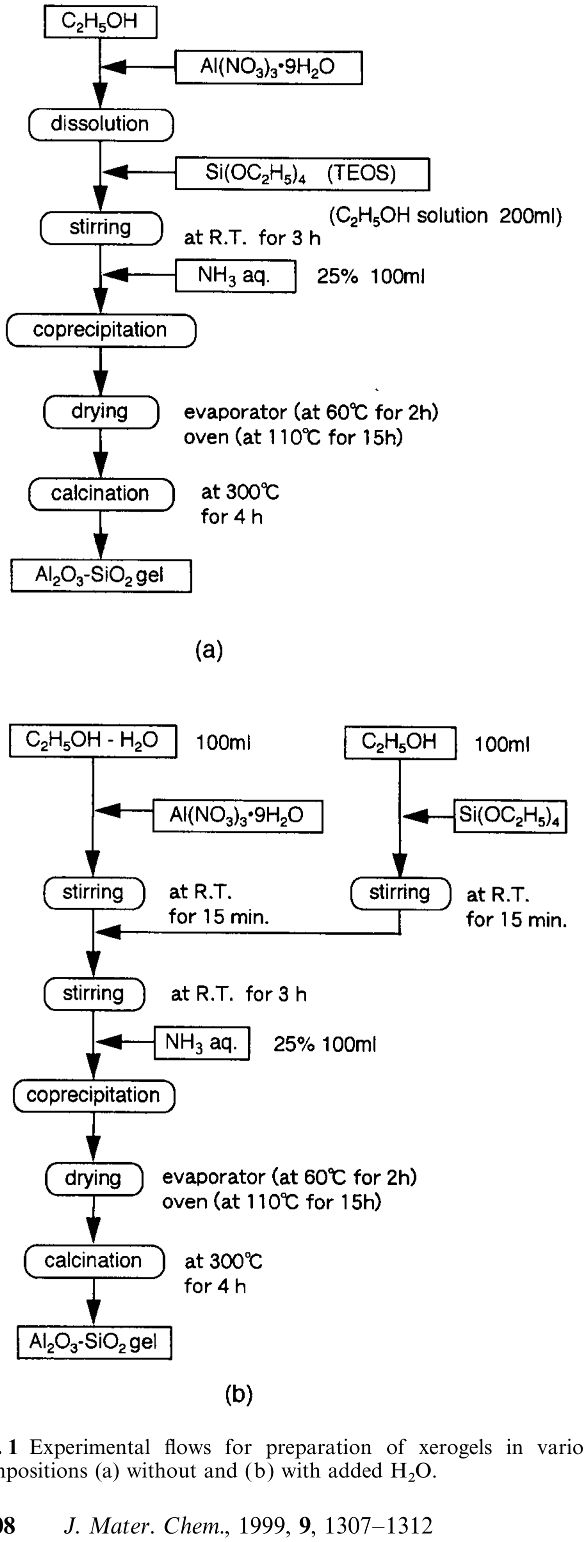

Fig. 1 Experimental flows for preparation of xerogels in various compositions (a) without and (b) with added H_2O.

In the preparations with added H_2O [Fig. 1(b)], measured amounts of distilled water and ethanol were mixed, ANN was added and the solution was stirred for 15 min. An ethanol solution containing a measured amount of TEOS was then added and stirred for 3 h. The xerogels were then obtained as for the preparations without added H_2O. The amount of H_2O in the solution was adjusted to give $H_2O/TEOS = 18/1$, this ratio indicating a large excess of H_2O for hydrolysis of TEOS. Since the amount of TEOS becomes smaller in the Al_2O_3 rich compositions, the H_2O/TEOS ratio exceeds 18/1 in the 80 and 100 mol% Al_2O_3 xerogels.

Characterization methods

The specific surface area (S_A) and total pore volume (V_P) were measured by the Brunnauer–Emmett–Teller (BET) method[12] using nitrogen gas as adsorbate at -196 °C with a Quanta Chrome Autosorb-1 instrument. The pore size distribution was calculated for a range of radii from 0.6 to 100 nm by the Barrett–Joyner–Halenda (BJH) method[13] using the desorption isotherm.

The particle size and microtexture of the agglomerated particles in the xerogels were observed by transmission electron microscopy (TEM) (Hitachi H9000 and JEOL 200CX instruments). The particle size in the xerogels was also examined using small angle X-ray scattering (SAXS) with a Rigaku RINT2500HF$^+$ instrument. Using the conventional method,[14] the radius of gyration (R_g) of scatterers in the xerogels was calculated from the slope ratio of the Guinier plot and the spherical equivalent radius (R_{sp}) was then evaluated from the corresponding R_g value.

Solid state ^{29}Si and ^{27}Al MAS NMR spectra were obtained at 11.7 T using a Varian Unity 500 spectrometer operating at ^{29}Si and ^{27}Al frequencies of 99.297 and 130.245 Hz with a 5 mm Doty MAS probe spun at 10–12 kHz. The ^{29}Si MAS spectra were obtained with a 7 ms 90° pulse and a delay time of 60 s, and acquired 400 scans. The ^{27}Al MAS spectra were obtained with a 1 ms 15° pulse and a delay time of 1 s, and acquired 2000–3000 scans (higher number of scans for low Al content samples). The ^{29}Si and ^{27}Al spectra were referenced to tetramethylsilane (TMS) and $Al(H_2O)_6{}^{3+}$, respectively.

Results

Xerogels prepared without added H_2O

Fig. 2–4 show the changes in specific surface area (S_A), total pore volume (V_P) and pore radius (r_P) of the aluminosilicate xerogels as a function of chemical composition. Fig. 2 shows that S_A varies with respect to the chemical composition, the change being especially marked in the SiO_2-rich xerogels. The maximum S_A of *ca.* 560 $m^2\ g^{-1}$ is obtained in the 9.4 mol% Al_2O_3 composition corresponding to that of silica–alumina catalysts generally used in industry. Values of S_A decrease very steeply with decreasing Al_2O_3 content from this composition and becomes $<10\ m^2\ g^{-1}$ at 0 mol% Al_2O_3. In the Al_2O_3-rich compositions, the xerogels maintain relatively high values of S_A, *i.e.* $>300\ m^2\ g^{-1}$ up to 100 mol% Al_2O_3. The xerogel with 50 mol% Al_2O_3 shows the maximum value of S_A (*ca.* 500 $m^2\ g^{-1}$) in this composition range.

Fig. 3 shows the change in V_P of the xerogels as a function of chemical composition. The behaviour of V_P with respect to chemical composition is a little different from that of S_A

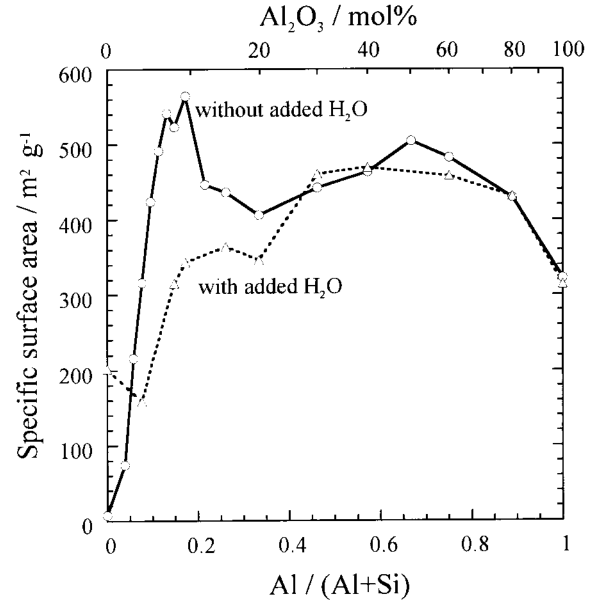

Fig. 2 Changes in specific surface areas (S_A) of the xerogels prepared with and without added H_2O as a function of chemical composition.

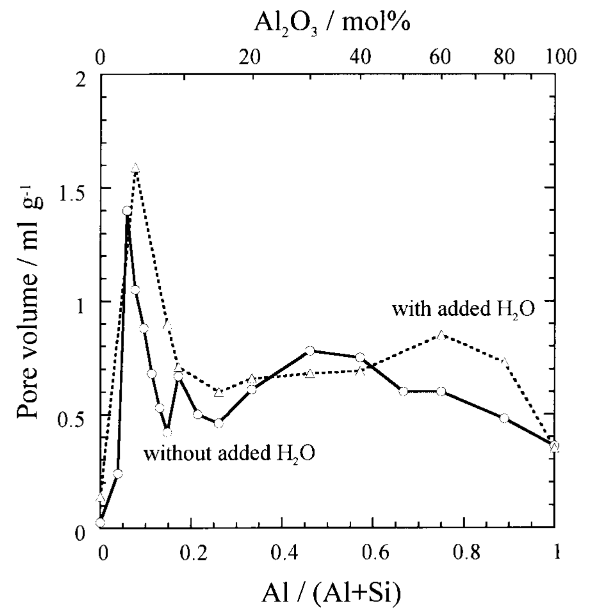

Fig. 3 Changes in total pore volumes (V_P) of the xerogels prepared with and without added H_2O as a function of chemical composition.

(Fig. 2). The xerogel shows a maximum V_P (≈ 1.4 ml g^{-1}) at 3 mol% Al_2O_3, peaking sharply at this composition, but showing a rather gentle change at Al_2O_3-rich compositions, with a broad peak at *ca.* 30 mol% Al_2O_3 The differences in composition dependence of S_A and V_P are related to changes in the pore size with chemical composition. As shown in Fig. 4, the pore radii (r_P) are *ca.* 2–3 nm over a wide chemical composition range (7–100 mol% Al_2O_3), showing a small broad peak at 30 mol% Al_2O_3 but increasing very steeply as the Al_2O_3 content decreases below 7 mol%, and reaching 34 nm at 3 mol%. This increase in r_P corresponds to a decrease in S_A and causes V_P to peak in the middle of this composition range as a result of the change in S_A and r_P.

Xerogels prepared with added H_2O

Values of S_A, V_P and r_P of the xerogels prepared with added H_2O are also shown in Fig. 2–4 as a function of chemical composition. In these preparations, S_A shows a plateau at *ca.* 30–80 mol% Al_2O_3 and decreases gradually on either side of this Al_2O_3 composition. No S_A peak is observed in these xerogels as is observed in those prepared without added H_2O (above). The S_A values obtained in the xerogels prepared with added H_2O (Fig. 2) are generally lower than those without added H_2O, with the exception of the value for 0 mol% Al_2O_3. The change of V_P with respect to the chemical composition of these xerogels (Fig. 3) is basically similar to that of the xerogels without added H_2O. The V_P values remain at *ca.* 0.6–0.8 ml g^{-1} as SiO_2 is introduced into the Al_2O_3 xerogel, but increase sharply as the Al_2O_3 content of the xerogels drops below 15 mol%, with a sharp peak at 4 mol% Al_2O_3. The maximum value of V_P (1.55 ml g^{-1}) is slightly larger than that for the sample without added water. The r_P values are *ca.* 3 nm (Fig. 4), and show little change with composition from 15–80 mol% Al_2O_3, but become larger as the Al_2O_3 content decreases below 15 mol% similar to the xerogels without added H_2O. The r_P values of these xerogels containing 4–15 mol% Al_2O_3 are much larger than those of the xerogels without added H_2O though the trends of r_P are similar.

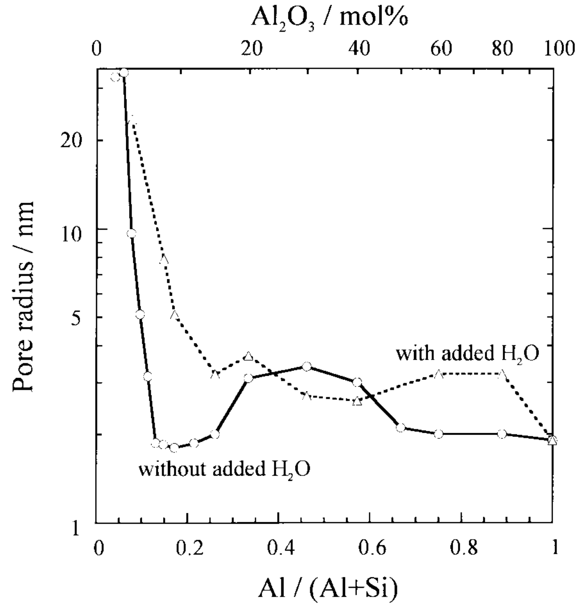

Fig. 4 Changes in pore radii (r_P) of the xerogels prepared with and without added H_2O as a function of chemical composition.

Discussion

The porous properties of the xerogels shown in Fig. 2–4 suggest that they may be divided into two groups, the change occurring at *ca.* 20 mol% Al_2O_3, irrespective of their preparation conditions. The porous properties of xerogels with Al_2O_3 $\geqslant$20 mol% show fairly small variations over a very wide chemical composition range while those with Al_2O_3 <20 mol% show a large variation with composition over a narrow composition range. In terms of the preparation conditions of these aluminosilicates, the precipitates are formed at pH ranging from strongly acidic to neutral. In general, the Al component precipitates as an aluminium hydroxide gel, which may contain some Si which does not precipitate at this pH. However, a silica sol is rapidly formed in solution by hydrolysis and/or polycondensation of TEOS when a large amount of aqueous ammonia solution is quickly added. The sol changes to a gel by further polycondensation in solution. The silica gel particles are believed to contain some Al. In the formation of these gel particles, a considerable incubation time is necessary for the transformation from the sol to the gel, although the addition of aqueous ammonia solution to SiO_2-rich solutions precipitates gel particles after only a couple of

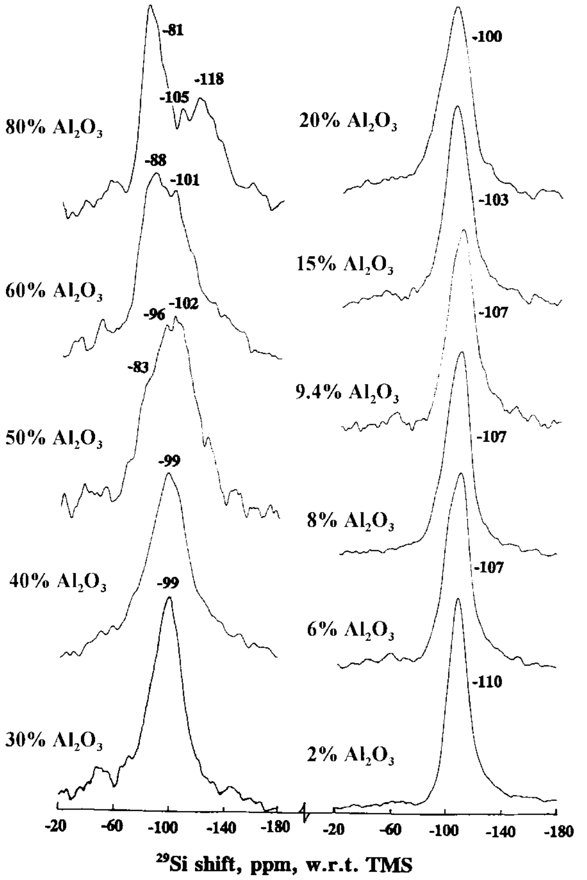

Fig. 5 ^{29}Si MAS NMR spectra of the xerogels prepared without added H_2O.

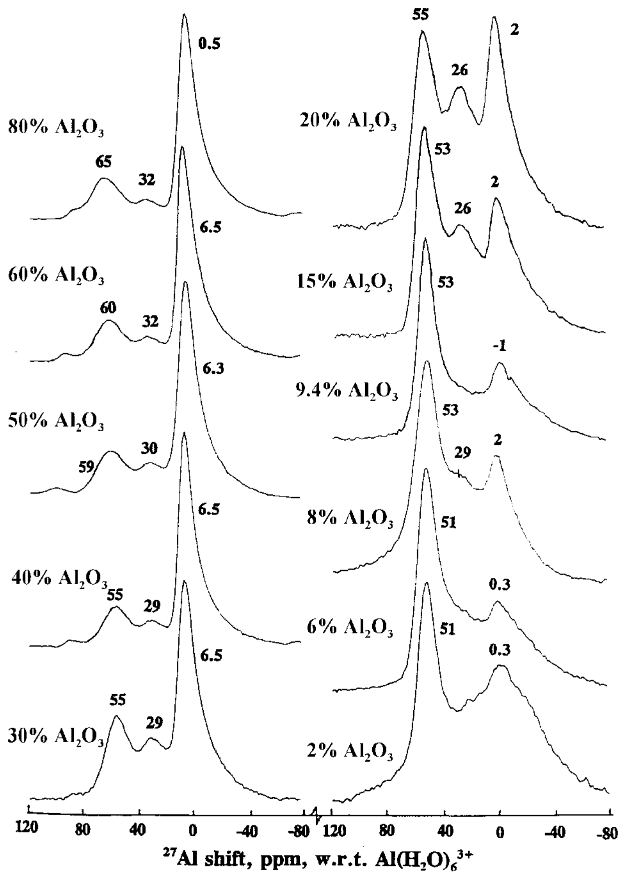

Fig. 6 ^{27}Al MAS NMR spectra of the xerogels prepared without added H_2O.

minutes. The incubation time for gel formation increases as the Al_2O_3 content in the solution decreases, but immediate precipitation can be obtained by the addition of aqueous ammonia solution to the Al_2O_3 rich gels.

The structure of the xerogels was characterized by ^{29}Si and ^{27}Al MAS NMR spectroscopy for samples of various compositions (Fig. 5 and 6). The ^{29}Si NMR spectra (Fig. 5) show a single peak ranging from -80 to -110 ppm, with some evidence of a dependence of peak position on the chemical composition. The ^{29}Si spectrum of the 2 mol% Al_2O_3 xerogel shows a single peak at -110 ppm, assigned to the structural unit Q^4 (SiO_4 tetrahedra in a framework structure). The peak positions gradually shift from -110 to *ca.* -100 ppm with increasing Al_2O_3 content up to 20 mol%. This change can be attributed to the incorporation of Al^{3+} in the framework structure SiO_4 tetrahedra. With increasing Al_2O_3 content, the resonance gradually broadens and assumes a complex shape arising from overlapping peaks. New peaks also appear at *ca.* -80 and -100 ppm in the spectra of the xerogels containing $\geqslant 50$ mol% Al_2O_3. The -80 ppm peak is considered to arise from tetrahedral Si surrounded by Al_2O_3, and may be merely adsorbed on the surface and/or incorporated in its structure. All the ^{27}Al NMR spectra (Fig. 6) show three peaks at *ca.* 0–7, 30 and 50–60 ppm. The peak at 0–7 ppm is assigned to octahedral Al and that at 50–60 ppm to tetrahedral Al. The peak at 30 ppm has been frequently described as five-coordinate Al but it could also arise from a distorted tetrahedral site.[15] The intensity ratios of the ^{27}Al peaks vary with sample composition. Up to 20 mol% Al_2O_3 the intensity of the tetrahedral Al peak is relatively stronger than that of octahedral Al though the ratio of tetrahedral to octahedral Al gradually decreases with increasing Al content. At compositions >20 mol% Al_2O_3, the intensity of the octahedral Al peak increases. In the Al_2O_3-rich xerogels, the intensity ratio also changes with chemical composition but the variation is very small compared with SiO_2-rich xerogels. This implies that most of the Al in these xerogels assumes the same structural state irrespective of the chemical composition. A plausible interpretation of these NMR data is that the xerogels consist of SiO_2-rich gel particles, which incorporate some Al^{3+} in the tetrahedral framework structure, together with Al_2O_3-rich gel particles, which may also contain some Si^{4+}.

Fig. 7 shows TEM photographs of the xerogels prepared with and without added H_2O. Photographs of the xerogels with 80 mol% Al_2O_3, indicate that most of the particles assume an elongated lath shape, suggesting that they are Al_2O_3-rich particles, which preserve the pseudomorphic particle shape of the original pseudoboehmite. With decreasing Al_2O_3 content, the elongated particles give way to fine spherical particles. With a further decrease in the Al_2O_3 content to <20 mol%, the fine particles agglomerate to form larger particles of submicrometer diameter, which eventually become one large smooth particle at 0 mol% Al_2O_3. The spherical particles are therefore considered to be SiO_2-rich, consistent with the structure of the xerogels deduced from the NMR data.

The size of scatterers, which correspond to the xerogel particles, was obtained by SAXS measurements. Table 1 lists the radius of gyration (R_g) and its equivalent spherical particle shape (R_{sp}) obtained from the SAXS analysis, together with the average particle size obtained by TEM (R_{TEM}). In the samples prepared without added H_2O, R_g varies in a complicated manner with the chemical composition of the xerogels, having a value of *ca.* 15 nm in the Al_2O_3-free sample, of relatively large size compared with the other xerogels. With increasing Al_2O_3 content, R_g decreases to 7.6 nm at 6 mol% Al_2O_3 before increasing to a maximum of 13 nm at *ca.* 8–10 mol% Al_2O_3. The value of R_g gradually decreases again to 6 nm at 80 mol% Al_2O_3. These R_g or R_{sp} values obtained by SAXS are in fair agreement with the R_{TEM} data. The TEM

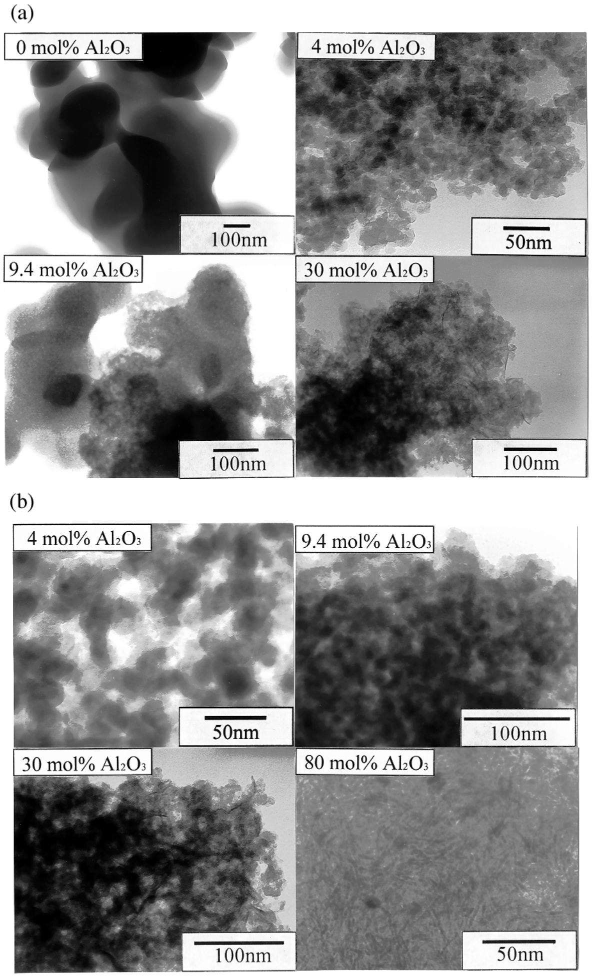

Fig. 7 TEM photographs of the xerogels prepared (a) without and (b) with added H_2O.

micrographs of the 8 and 9.4 mol% Al_2O_3 xerogels show large submicrometer particles and very fine nanometer sized particles. The presence of the large particles explains the increased R_g of these xerogels. On the other hand, R_g and R_{TEM} of the xerogels with added H_2O show a monotonic decrease with increasing Al_2O_3 content. The particles in these xerogels are seen to be a mixture of fine spherical particles(SiO_2-rich) and lath-shaped particles (Al_2O_3-rich).

The pores in the xerogels are formed in the spaces between the fine agglomerated particles as seen in Fig. 7. The relation between the size of the particles and the spaces can be deduced from simple geometrical models, *i.e.* pores are formed in tightest packing by three particles and in loosest packing by four particles. If the spaces are assumed to be formed by agglomerations of either three or four particles, the size of particles which form pores of 2 and 3 nm radius are calculated to be 13 and 19 nm for a three particle agglomeration, and 5 and 7 nm for a four particle agglomeration. These calculated particle sizes are comparable with those observed in the xerogels, suggesting that the pores of 2–3 nm radius correspond to the spaces formed by agglomeration of these particles. On the other hand, the pore size increased with decreasing Al_2O_3 content (Fig. 4), although, the size of the primary particles in these xerogels does not increase as much as the increase in the pore size. We therefore believe that another type of agglomerated structure may be responsible for the larger pores formed in the SiO_2 rich xerogels.

There is a clear difference in the porous properties of xerogels prepared with and without added H_2O in the SiO_2 rich compositions discussed above. This must be related to the H_2O in the solutions because the amount of H_2O in the samples prepared without added H_2O is insufficient for complete hydrolysis of TEOS before precipitation. Fig. 8 shows the pore size distributions of the xerogels. These data also clearly show a change in behaviour at 20 mol% Al_2O_3; at higher contents there is little variation in the pore size distribution over a wide composition range, but below this Al_2O_3 content a greater variation is apparent over a narrow composition range. The changes in the pore size distributions of these xerogels as a function of composition is similar in the samples

Table 1 Particle size of the xerogels derived from SAXS and TEM[a]

Al_2O_3 (mol%)	Without added H_2O R_g/nm	R_{sp}/nm	R_{TEM}/nm	With added H_2O R_g/nm	R_{sp}/nm	R_{TEM}/nm
0	15	19	—	—	—	—
2	13	17	—	—	—	—
3	12	15	—	—	—	—
4	9.8	12	12	12	15	13
5	7.7	10	—	—	—	—
6	7.6	10	—	—	—	—
7	8.1	11	—	—	—	—
8	13	16	20, 270	8.1	10	8
9.4	13	16	11, 100	8.4	11	8
30	8	10	13	7.4	10	6
80	6	8	4	6.3	8	4

[a] R_g = radius of gyration obtained from SAXS, R_{sp} = radius equivalent to spherical particle shape calculated from R_g, R_{TEM} = average radius obtained from TEM.

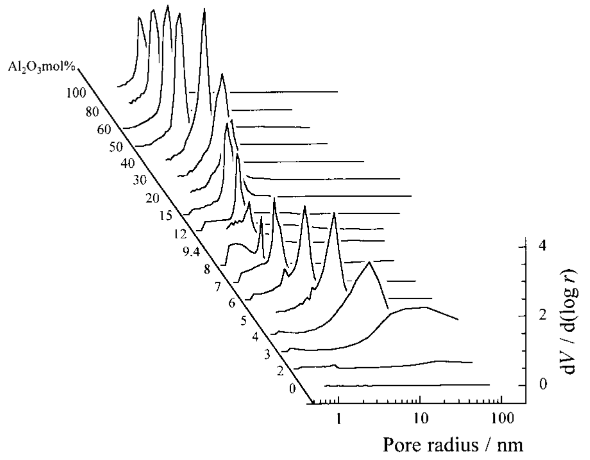

(a) Without added H_2O

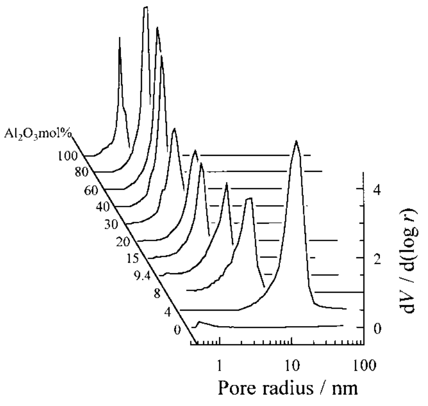

(b) With added H_2O

Fig. 8 Pore size distributions of the xerogels prepared (a) without and (b) with added H_2O.

prepared both with and without added H_2O (Fig. 4). However, differences occur in the pore size distributions in the region <2 nm; xerogels containing 8–10 mol% Al_2O_3 show a bimodal pore size distribution in the samples prepared without added H_2O but not in samples prepared with added H_2O. Since the newly formed pores are microporous, the S_A values of these xerogels increase, as shown in Fig. 2. The TEM micrographs (Fig. 7) show differences in the microtexture of the xerogels prepared with and without added H_2O; the microtexture of xerogels prepared with added H_2O is uniform and consists of agglomerated fine spherical particles whereas the microtexture of samples prepared without added H_2O is inhomogeneous. One part of the microtexture consists of agglomerates of very large particles of submicrometer size but a second microtexture contains agglomerates of very fine particles. The micropores are considered to be formed in the spaces of this microtexture. The fine particles may be formed at a particular H_2O/TEOS ratio in the preparation of these xerogels. The size of the primary particles in the product becomes slightly larger with increasing SiO_2 content. In these samples, the degree of hydrolysis and polycondensation of the Si component may decrease with increasing SiO_2 content because the amount of H_2O in the solution decreases, causing rapid polycondensation of the Si component when precipitation is induced by addition of NH_3 (aq). Since this reaction occurs under alkaline conditions, the particles become relatively large, especially in the samples without Al_2O_3, prepared without added H_2O. The pore size in this xerogel is too large to measure by gas adsorption, indicating a radius of up to 100 nm.

Conclusion

Amorphous aluminosilicates with various chemical compositions were prepared by coprecipitation from an ethanol solution containing calculated amounts of TEOS and ANN. The effect of chemical composition and the addition of H_2O on their porous properties was investigated, with the following results.

(1) The porous properties of these xerogels showed variations in the specific surface area of *ca.* 10–560 $m^2\,g^{-1}$, with variations in the total pore volume of *ca.* 0.02–1.6 ml g^{-1} and variations in the pore radius of *ca.* 2–34 nm.

(2) The greatest variation in the porous properties occurred in SiO_2-rich xerogels composition (0–20 mol% Al_2O_3) but only small variations were found in the Al_2O_3-rich compositions (20–100 mol% Al_2O_3).

(3) The xerogels are considered to consist of a mixture of SiO_2-rich and Al_2O_3-rich particles. Some incorporation of Al^{3+} in the SiO_4 tetrahedra of the SiO_2-rich particles was indicated by ^{29}Si and ^{27}Al MAS NMR spectroscopy.

(4) Addition of H_2O strongly influenced the porous properties of the SiO_2-rich xerogels.

(5) Pores of *ca.* 2–3 nm radius are formed in the spaces between agglomerates of fine particles up to 20 nm in size but the larger pores observed in the SiO_2 rich xerogels are formed by the synergetic agglomerated structure of similar-sized particles.

Acknowledgements

We are grateful to Professor T.Yano of Research Laboratory for Nuclear Reactor, Tokyo Institute of Technology and also to Mr. R.Ooki of Tokyo Institute of Technology for TEM observation.

References

1 I. J. Maxwell and W. H. J. Stork, *Stud. Surf. Sci. Catal.*, 1991, **58**, 571.

2 S. D. Jones, T. N. Pritchard and D. F. Lander, *Micropor. Mater.*, 1995, **3**, 419.

3 A. C. Pierre, *Ceram. Int.*, 1997, **23**, 229.

4 J. Zaman and A. Chakma, *J. Membr. Sci.*, 1994, **92**, 1.

5 K. Okada, T. Tomita and A. Yasumori, *J. Mater. Chem.*, 1998, **8**, 2863.

6 H. Schneider, K. Okada and J. A. Pask, *Mullite and Mullite Ceramics*, John Wiley, Chichester, 1994.

7 M. May, M. Asomoza, T. Lopez and R. Gomez, *Chem. Mater.*, 1997, **9**, 2395.

8 B. M. De Witte and J. B. Uytterhoeven, *J. Colloid Interface Sci.*, 1996, **181**, 200.

9 F. Hayashi, K. Takei, Y. Machi and T. Shimazaki, *J. Ceram. Soc. Jpn.*, 1990, **98**, 663.

10 S. Inagaki, Y. Fukushima, A. Okada, T. Kurauchi, K. Kuroda and C. Kato, in *Proc. 9th Int. Zeolite Conf.* ed. R. von Ballmoos *et al.*, Reed Publishing, 1993, p. 305.

11 B. M. De Witte, K. Aernouts and J. B. Uytterhoeven, *Micropor. Mater.*, 1996, **7**, 97.

12 S. Brunauer, P. H. Emmett and E. Teller, *J. Am. Chem. Soc.*, 1938, **60**, 309.

13 E. P. Barrett, L. G. Joyner and P. P. Halenda, *J. Am. Chem. Soc.*, 1951, **73**, 373.

14 H. Boukari, J. S. Lin and M. T. Harris, *Chem. Mater.*, 1997, **9**, 2376.

15 M. Schmucker and H. Schneider, *Ber. Bunsen-ges Phys. Chem.*, 1996, **100**, 1550.

Paper 9/00611G